Carbon dioxide sequestration by direct mineral carbonation: process mineralogy of feed and products

W.K. O'Connor, D.C. Dahlin, G.E. Rush, C.L. Dahlin and W.K. Collins
Geologist, metallurgist, engineering technician, geologist and metallurgist, respectively, Albany Research Center, Office of Fossil Energy, US Department of Energy, Albany, Oregon

Abstract

Direct mineral carbonation was investigated as a process to convert gaseous CO_2 into a geologically stable final form. The process utilizes a slurry of water, with bicarbonate and salt additions, mixed with a mineral reactant, such as olivine (Mg_2SiO_4) or serpentine [$Mg_3Si_2O_5(OH)_4$]. Carbon dioxide is dissolved into this slurry, resulting in dissolution of the mineral and precipitation of magnesium carbonate ($MgCO_3$). Optimum results were achieved using heat-pretreated serpentine feed material and a high partial pressure of CO_2 (P_{CO_2}). Specific conditions include 155°C, $P_{CO_2} = 185$ atm and 15% solids. Under these conditions, a 78% conversion of the silicate to the carbonate was achieved in 30 minutes. Process mineralogy was utilized to investigate the appropriate feed characteristics, identify the process products and interpret the mineral dissolution and carbonate precipitation reaction paths.

Key words: Mineral carbonation, Carbon dioxide sequestration, Carbonates

Introduction

During the past two years, the Albany Research Center (ARC) of the US Dept. of Energy (DOE) has been conducting mineral carbonation tests at its Albany, Oregon, facility as part of a Mineral Carbonation Study Program within the DOE. Other participants in this Program include the Los Alamos National Laboratory (LANL), Arizona State University (ASU), Science Applications International Corp. (SAIC) and the DOE National Energy Technology Laboratory (NETL).

Lackner, et al. (1996) and Lackner et al. (1997) discussed CO_2 storage as mineral carbonates in prior literature, although these publications describe a process that differs dramatically from the subject process. The direct mineral carbonation process utilizes a slurry of fine mineral particles in water at solids concentrations ranging from 15% to 30%. The dissolution of the mineral and the subsequent carbonation occur in a single unit operation. The theorized reaction equations are

$$CO_2 + H_2O \rightarrow H^+ + HCO_3^- \qquad (1)$$

$$Mg_2SiO_4 + 4H^+ \rightarrow 2Mg^{+2} + SiO_2 + 2H_2O \qquad (2)$$

$$Mg^{+2} + HCO_3^- \rightarrow MgCO_3 + H^+ \qquad (3)$$

The CO_2 is dissolved in water to form carbonic acid (H_2CO_3), which dissociates to H^+ and HCO_3^- (Eq. (1)). The H^+ ion hydrolyzes the mineral, liberating Mg^{+2} cations and forming silicic acid or free silica and water (Eq. (2)). The free Mg^{+2} cations react with the bicarbonate ions to form the solid carbonate (Eq. (3)). A potential process flow diagram is shown in Fig. 1. The process was described in detail in O'Connor et al. (1999) and in O'Connor et al. (2000).

Modifications to the carbonation solution chemistry were also investigated. Additions of $NaHCO_3$ and NaCl to the solution improved the reaction rate dramatically. It is theorized that the bicarbonate ion reacts with the silicate forming the carbonate, hydroxide (OH^-) ions and free silica (SiO_2) by the following reaction

$$Mg_2SiO_4 + 2HCO_3^- \rightarrow 2MgCO_3 + SiO_2 + 2OH^- \qquad (4)$$

The OH^- ion is believed to react immediately with the additional CO_2 being injected into the solution to reform the bicarbonate, maintaining a relatively constant solution chemistry, as follows

$$OH^- + CO_2 \rightarrow HCO_3^- \qquad (5)$$

This may be described as a buffered solution. The in situ pH of the solution cannot be measured, but pre- and post-test pH measurements remain relatively constant in the range of 7.7 to 8.0. This supports the assertion that the solution chemistry remains relatively constant and verifies that the bicarbonate addition is not consumed in the reaction but acts as a catalyst.

Thus far, the direct mineral carbonation tests have focused on ultramafic minerals as the primary reactants. Geologic studies by Hunter (1941), the IGCP (1977), Goff et al. (1997) and Goff et al. (2000) indicate that reserves of these ultramafic minerals are sufficient to provide raw materials for the mineral carbonation of all annual CO_2 emissions for many years. Additional studies conducted at ARC indicate that the mining and milling costs necessary to prepare the minerals for the ex situ process would be similar to those in the porphyry copper mining industry, at approximately \$4 to \$5 per ton. Estimates were made concerning the tonnage of silicate mineral necessary to carbonate 100% of the CO_2 emissions from a single 1-GW coal-fired power plant. Assuming a mean MgO content of the silicate ore of 45% (by weight), 100% ore recovery and 80% efficiency of the

Preprint number 01-091, presented at the SME Annual Meeting, Feb. 26-28, 2001, Denver, Colorado. Original manuscript accepted for publication February 2001. Discussion of this peer-reviewed and approved paper is invited and must be submitted to SME Publications Dept. prior to Nov. 30, 2002.

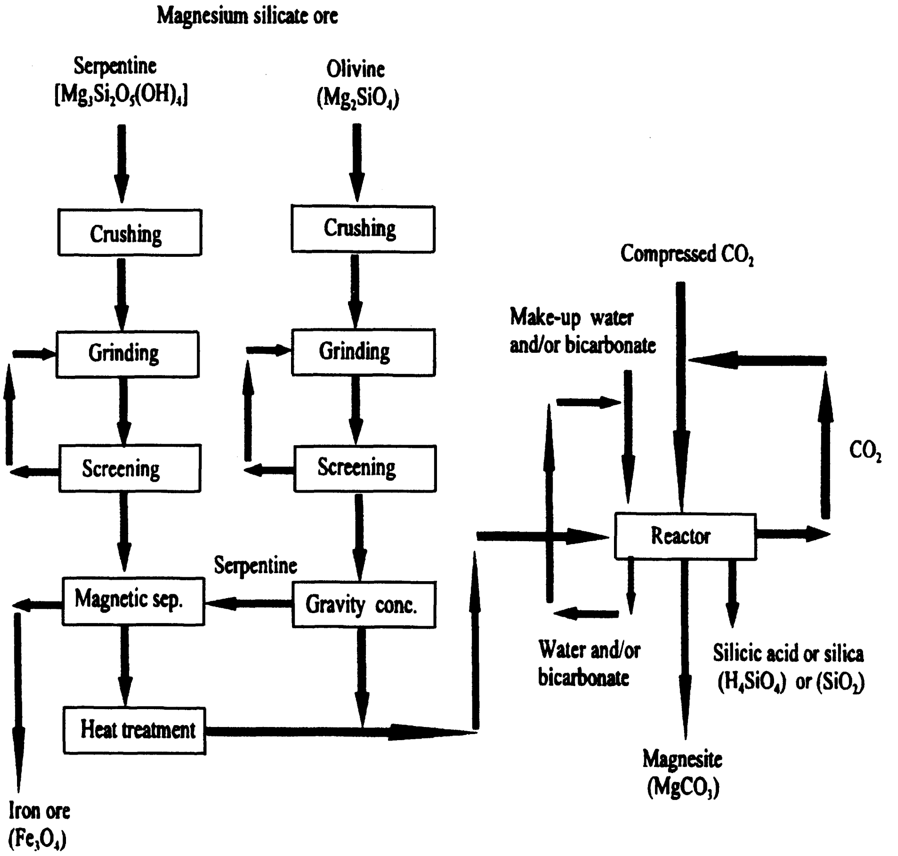

Figure 1 — Process flow diagram for the direct mineral carbonation process.

carbonation reaction, a 1-GW coal-fired power plant generating approximately 20 kt/day CO_2 would require more than 40 kt/day of ore.

Materials

Several magnesium silicate minerals are suitable for the ex situ carbonation reaction, including serpentine [$Mg_3Si_2O_5(OH)_4$], enstatite ($MgSiO_3$), and olivine, which actually represents a mineral group encompassing the solid-solution series between magnesium-rich (forsterite, Mg_2SiO_4) and iron-rich (fayalite, Fe_2SiO_4) end members. Each of these minerals occurs in ultramafic complexes, several of which are well documented in North America. Serpentine is an alteration product of olivine and other magnesium silicates and occurs in huge deposits on both the east and west coasts of North America (Goff et al., 1997). Olivine, particularly the forsterite end member, is also found in huge deposits on both coasts (Hunter, 1941; IGCP, 1977), although not to the extent of serpentine. Both minerals constitute potential feedstock for the mineral carbonation process, but a magnesium silicate mineral of high purity, low water content and high MgO concentration is preferred. Because serpentine is a hydrated mineral and contains a lower molar concentration of MgO than olivine, the latter mineral was selected for the initial series of direct carbonation tests. Following these tests, during which basic reaction parameters were established, serpentine was included. Heat pretreatment, necessary to remove the chemically bonded water from the serpentine, was found to activate the mineral, resulting in a reaction rate exceeding that for olivine. However, the energy demand may preclude heat treatment. Therefore, alternative means to activate the serpentine are under investigation. The chemical compositions of the typical olivine, serpentine and heat-treated serpentine head samples are included in Table 1.

The magnesium oxide contents of the olivine and serpentine head samples were measured at 49.7% and 40.8% (by

Table 1 — Chemical composition of the feed and products (weight percent)

	Olivine (forsterite)	Serpentine	Heat-treated serpentine	SC-4 product	SC-11 product	SC-25 product	SC-39 product	SC-40 product	SC-84 product
Oxide:									
Al_2O_3	0.208	0.167	0.270	0.171	0.149	0.171	0.196	0.132	0.180
CaO	0.070	0.077	0.146	0.155	0.155	0.230	0.356	0.231	0.022
Cr_2O_3	0.044	NA	NA	NA	NA	NA	NA	0.247	NA
FeO	5.966	3.497	3.394	5.953	6.223	5.271	0.386	8.576	2.649
Fe_2O_3	2.558	3.272	4.544	NA	0.029	NA	4.973	<0.010	3.301
MgO	49.677	40.842	45.676	41.675	40.508	35.507	33.673	36.841	27.672
K_2O	0.007	0.003	0.004	NA	NA	NA	0.006	0.005	0.006
SiO_2	41.357	36.214	40.500	33.214	32.571	26.786	28.701	26.357	29.786
Na_2O	0.099	0.010	0.010	NA	NA	NA	0.414	0.144	0.492
Volatiles:									
C, CO_2	<0.300	0.460	0.290	17.700	19.800	32.300	28.071	29.800	24.700
C, fixed	0.021	0.020	0.017	0.033	0.060	3.691	0.584	0.213	0.014
H_2O^1	0.380	0.310	0.680	NA	NA	NA	0.200	<0.050	0.700
H_2O^2	0.000	13.610	3.203	NA	NA	NA	1.516	0.687	2.886
Total:	100.387	98.482	98.734	98.902	99.496	103.956	98.575	100.487	92.407

[1] Water of dehydration (free moisture).
[2] Chemically-bonded (interstitial) water.

NA = Not analyzed

Table 2 — Test summaries for the direct mineral carbonation tests.

Test	Feed material	Particle size µm	Carbonation conditions Time, hr	Temp., °C	P_{CO_2}, atm	Solution chemistry	Stoich. conv. %
SC-4	olivine	53 x 37	24	185	115	distilled water	52
SC-11	olivine	53 x 37	48	185	115	distilled water	56
SC-25	olivine	-37	24	185	115	distilled water	91
SC-39	serpentine[1]	-37	6	185	115	0.5 M $NaHCO_3$, 1 M NaCl	83
SC-40	olivine	-37	6	185	115	0.5 M $NaHCO_3$, 1 M NaCl	84
SC-84	serpentine[1]	-37	0.5	155	185	0.64 M $NaHCO_3$, 1 M NaCl	78

[1]Heat treated serpentine.

weight), respectively. The difference is largely attributable to the high concentration of chemically bonded water (13.6% by weight) in the serpentine. The serpentine was heat treated for two hours at 630°C to remove the water, resulting in a subsequent increase in magnesium oxide content to 45.7% (by weight). Emphasis is placed on the magnesium oxide concentration of the feed material because it is this oxide that reacts with the carbon dioxide to form the carbonate. Thus, feed materials with higher magnesium oxide concentrations are preferred. Calculation of the extent of reaction for the direct carbonation tests was based on the concentration of magnesium oxide in the appropriate feed material and the stoichiometry of the following theoretical equations

$$Mg_2SiO_4 + 2CO_2 \rightarrow MgCO_3 + SiO_2 \qquad (6)$$

$$Mg_3SiO_5(OH)_4 + 3CO_2 \rightarrow 3MgCO_3 + 2SiO_2 + 2H_2O \qquad (7)$$

Experimental procedures

The initial proof-of-concept tests were conducted in an autoclave with continuous agitation or stirring, while process parameters were monitored and recorded in real time. The stirred-tank reactor (STR) was prepared for operation by the following procedure:

- 100 g of olivine is placed into the STR;
- 400 mL of distilled water is poured into the STR;
- the STR is sealed, evacuated, weighed (tare weight) and placed into an ice bath;
- liquid CO_2 is introduced into STR;
- the STR is placed back on the scale and the weight of CO_2 is determined;
- with the STR on the scale, pressure is bled off until the proper weight of CO_2 remains;
- the STR is heated to the final process temperature and pressure;
- after the specified test time, the STR is cooled, the pressure is bled off and the slurry is removed; and
- the slurry is filtered, the solids are dried, weighed and sampled for analysis, and the solution is sampled for analysis.

The proper weight of CO_2 was calculated in advance using the compressibility factor equation of state

$$P\hat{V} = zRT \qquad (8)$$

where
P is the pressure (atm),
$\hat{V}$ is the molar volume (mole/L),
z is the compressibility factor for CO_2,
R is the gas constant ($L{\cdot}atm{\cdot}mole^{-1}{\cdot}K^{-1}$) and
T is the temperature (K).

The solubility of CO_2 in water at the desired conditions was also included in the final calculation. A detailed description of the procedure is included in a previous paper (O'Connor et al., 1999).

Following the initial test series, a new autoclave system (STR) was developed, including a CO_2 gas-booster pump controlled by a pressure transducer on the autoclave. The modified test procedure is

- 167 g of mineral reactant and 950 g of distilled water (or bicarbonate/salt solution) are poured into the STR;
- the STR is sealed, purged with CO_2 and stirred at 1,000 rpm;
- the STR is heated to the final operating temperature with the stirrer speed increased to 2,000 rpm;
- CO_2 is injected to the final operating pressure;
- additional CO_2 is injected as the system pressure decreases due to the chemical reactions and/or due to pressure leaks;
- after the specified test time, the STR is cooled, the pressure is bled off, and the slurry is removed;
- the slurry is filtered, the solids are dried, weighed and sampled for analyses, and the solution is sampled for analyses.

All tests conducted in the new system followed this simplified procedure. The inclusion of the gas booster pump permitted operation under relatively constant P_{CO_2}, which was not possible in the former system. This minimized the impact of decreasing P_{CO_2} on the reaction rate and final extent of reaction.

Experimental results

Olivine carbonation. The initial series of olivine carbonation tests included no pretreatment options other than size reduction to the desired particle size. These tests, exploratory in nature, were intended to produce a baseline set of test parameters for the carbonic acid process, utilizing distilled water as the liquid medium and continuous agitation of the slurry. The extent of reaction achieved in the 24- and 48-hour tests were 52% and 56% stoichiometric, respectively (Table 2, Tests SC-4 and 11). The extent of reaction, and possibly the reaction rate, decreased with decreasing P_{CO_2}. The addition of gas dispersion in the water column and the ability to operate at constant P_{CO_2} (in the new autoclave system) resulted in significant improvement in the extent of reaction. This culminated in 91% stoichiometric conversion of the silicate to the carbonate in 24 hours, at a temperature of 185°C and P_{CO_2} of 115 atm (Table 2, Test SC-25). Formation of the carbonate was confirmed by the identification of magnesite ($MgCO_3$) in the reaction products by X-ray diffraction (XRD) analysis (Table 3).

Serpentine carbonation. During investigations conducted on naturally occurring serpentine, it was demonstrated that

Table 3 — X-ray diffraction analyses for the feed and products.

Test	Material	Primary	Secondary	Minor	Trace
SC-4	olivine head	forsterite	–	enstatite	–
	carbonation product	magnesite	forsterite	–	enstatite
SC-11	olivine head	forsterite	–	enstatite	–
	+30-µm product	forsterite	–	enstatite	–
	30 x 10-µm product	forsterite	–	–	magnesite, enstatite
	-10-µm product	magnesite	–	–	forsterite
SC-25	olivine head	forsterite	–	enstatite	
	carbonation product	magnesite	–	–	forsterite, enstatite
SC-39	serpentine head	antigorite	–	clinochrysotile	magnetite, clinochlore
	heat treat product	forsterite	–	magnetite, antigorite	–
	carbonation product	magnesite	–	–	magnetite, forsterite, antigorite
SC-40	olivine head	forsterite	–	enstatite	–
	carbonation product	magnesite	–	forsterite	enstatite, antigorite (?)
SC-84	serpentine head	antigorite	–	clinochrysotile	magnetite, clinochlore
	heat treat product	forsterite	–	magnetite, antigorite	–
	carbonation product	magnesite	–	–	magnetite, forsterite

Key:
Primary phase: 40% to100%
Secondary phase: 20% to 60%
Minor phase: 5% to 30%
Trace phase: 0% to 10%

Minerals equations:
antigorite = $[Mg_3Si_2O_5(OH)_4]$
clinochlore = $(Mg_5Al_2Si_3O_{14}4H_2O)$
clinochrysotile = $[Mg_3Si_2O_5(OH)_4]$
enstatite = $(MgSiO_3)$
forsterite = (Mg_2SiO_4)
magnesite = $(MgCO_3)$
magnetite = (Fe_3O_4)

heat treating the serpentine, to remove chemically bonded water and activate the mineral, improved the carbonation results (Table 2, Tests SC-39 and SC-84). The reaction rate for serpentine carbonation was continuously improved by slight reductions of the reaction temperature, increases in the P_{CO_2} and additional modifications of the solution chemistry. The optimum reaction conditions identified to date for heat-treated serpentine include a sodium bicarbonate and sodium chloride solution chemistry and the reaction temperature of 155°C at a P_{CO_2} of 185 atm. These conditions resulted in serpentine carbonation to approximately 78% of the stoichiometric maximum in 0.5 hours (Table 2, Test SC-84). Magnesite was again identified by XRD as the primary phase in the reaction products (Table 3).

Analysis and discussion of results

Chemical analyses were acquired for the solid products from each of the carbonation tests and are reported in Table 1. The CO_2 concentration in the products, coupled with the identification of magnesite by XRD provided conclusive evidence that the mineral-carbonation process was successful. However, understanding the pathway to this final product required further characterization. Several important questions remained unanswered, such as:

- does the conversion of the silicate to carbonate occur in the solid state,
- what is the primary mechanism for carbonate formation,
- what intermediate products occur,
- is the reaction strictly surface controlled or is it diffusion limited,
- is the reaction inhibited by the formation of passive coatings on the particles and
- what is the fate of the silica?

Samples of the product solids were prepared for examination with the scanning electron microscope (SEM) with wavelength-dispersive X-ray microanalysis (WDX). The results from the SEM studies provided insight regarding the reaction pathways that occur in the direct mineral-carbonation process and provide answers to several of the questions posed above. An examination of specific test products led to an improved understanding of the reaction pathway, although the results are not yet definitive. The discussion is grouped by carbonation test.

SC-4 olivine reaction products. The product solids from carbonation test SC-4 are depicted in Fig. 2, which includes (a) a backscatter-electron (BSE) image and (b), (c) and (d) X-ray maps for Si, Mg and O, respectively). Although the X-ray maps are elemental, it is assumed that they are representative of the oxide species, unless otherwise noted. The majority of the large particles were identified as forsterite, with a few enstatite grains, reflective of the concentrations for these phases identified by XRD (Table 3).

The fine-grained (<10-µm) particles dispersed throughout the mount were identified as magnesite by SEM-WDX. This is clearly indicative of carbonate precipitation, rather than solid-state conversion, as the predominate mechanism for carbonate formation. Comparison of the X-ray maps for Mg and O with the BSE image show that the majority of the fine particles include Mg and O, but Si is virtually absent. This is significant when considering the final fate of the silica

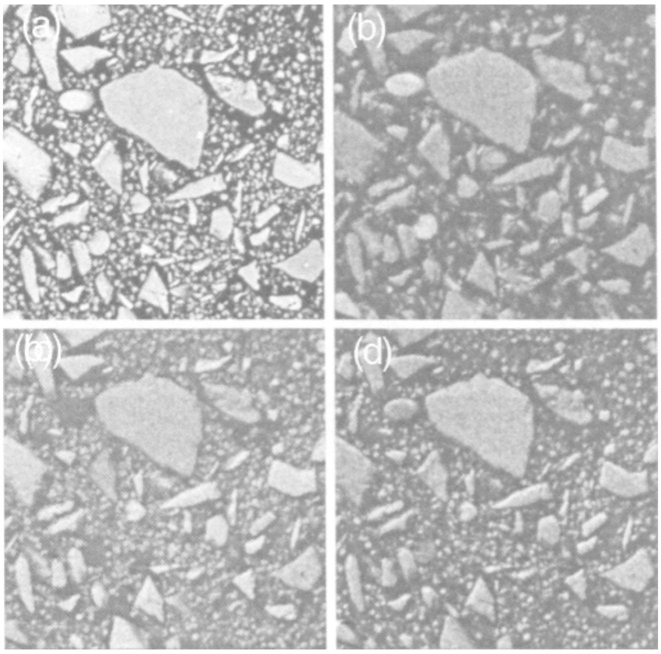

Figure 2 — (a) BSE image of SC-4 product (1,500x) and (b), (c) and (d) X-ray maps for Si, Mg and O on SC-4 product, respectively.

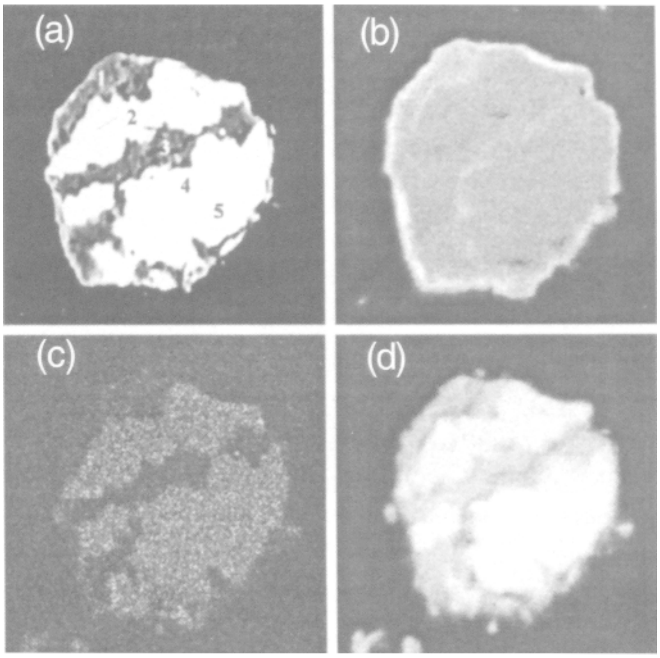

Figure 3 — (a) BSE image of SC-11 product (2,000x) and (b), (c) and (d) X-ray maps for Si, Fe and Mg on SC-11 product, respectively.

originating from the silicate mineral. The silica does not appear to agglomerate with or precipitate onto the magnesite particles.

SC-11 olivine reaction products. The effect of silica transport on the reaction rate can be significant. The concentration of free silica increases with increased extent of reaction, thus, the fate of this silica is important. Figure 2 suggests that silica does not accumulate in the magnesite precipitate — what is the fate of the silica? Residual silica may not be transported at all. This would result in silica-enriched zones (as the Mg^{+2} cation is removed) within the original silicate grains. The series of photomicrographs in Fig. 3, including (a) a BSE image and (b), (c) and (d) X-ray maps for Si, Fe and Mg, respectively, provide insight regarding the silica occurrence in the reaction products.

The Si X-ray map clearly shows a bright border on the surface of the silicate particles and lining the cracks within the silicate particles. This suggests that a silica-rich layer coats the reactive surface, possibly inhibiting further dissolution. Armoring of the silicate particles by a silica-rich layer could slow any further chemical attack. This suggests that the reaction may be diffusion limited.

The Fe and Mg X-ray maps clearly show two distinct zones within the silicate particle. Figure 3(c) shows an Fe-rich zone (bright white dots) and an Fe-depleted zone (black areas of particle). Figure 3(d) shows that the Mg concentration in the same two zones mirrors that of the Fe, with high Mg concentration in the bright white zones. This could be indicative of alteration. Removal of Fe^{+2} and Mg^{+2} cations by the carbonation solution could explain the disparity in concentration of these two metals between the two zones. The Si X-ray map shows a relatively uniform Si concentration throughout the particle, suggesting that the cations are removed without mobilization of the silica. A series of point scans, numbered 1 through 5 on Fig. 3(a), were compiled to examine the concentration of Fe, Mg, O and Si in these distinct zones (Table 4).

Table 4 — SEM-WDX microanalyses for SC-11 product.

	Atomic percent				
Point	**Fe**	**Mg**	**O**	**Si**	**Mg/Si**
1	ND	17	65	17	1.0
2	1.5	26	59	13	2.0
3	ND	19	66	15	1.3
4	2	26	59	13	2.0
5	2	26	59	13	2.0
Fo	0	28.6	57.1	14.3	2.0
En	0	20	60	20	1.0

ND = Not detected

Theoretical compositions for forsterite (Fo) and enstatite (En) are included in Table 4. Points 2, 4 and 5 have a Mg/Si ratio of 2:1, equal to that of forsterite, the primary feed mineral. These portions of the grain, which essentially appear free of fractures and isolated from the outer surface, have apparently undergone little or no alteration. However, Points 1 and 3 have much lower Mg/Si ratios of 1:1 and 1.3:1, respectively. Are the zones corresponding to Points 1 and 3, which occur at the particle surface and/or along fractures within the particle, indicative of alteration or could this two-phase grain be an unaltered fragment of the feed?

Examination of the olivine feed for test SC-11 does identify similar two-phase, forsterite-enstatite grains. Iron content is lower in the enstatite compared to the forsterite as well. However, the complete absence of Fe in the zones corresponding to Points 1 and 3 (Fig. 3 (a)) is unusual, and argues the point that some alteration is evident. Examination of reaction products from tests with greater extent of reaction than test SC-11 (56% stoichiometric conversion) is necessary to more positively identify the alteration products.

Test SC-11 was a 48-hour test. This longer duration test

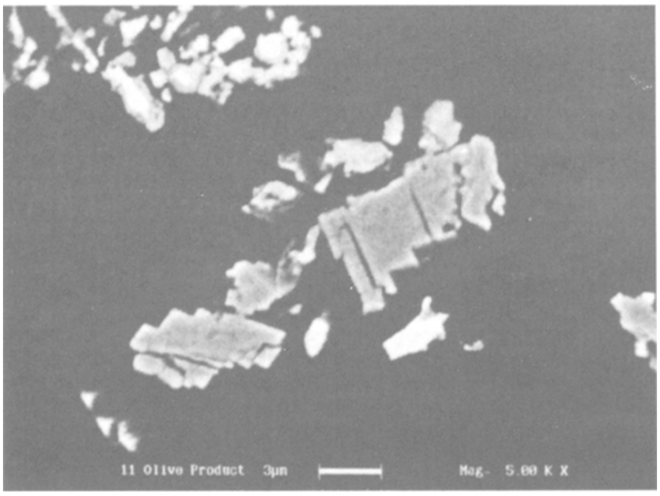

Figure 4 — Rhombohedral magnesite in SC-11 product.

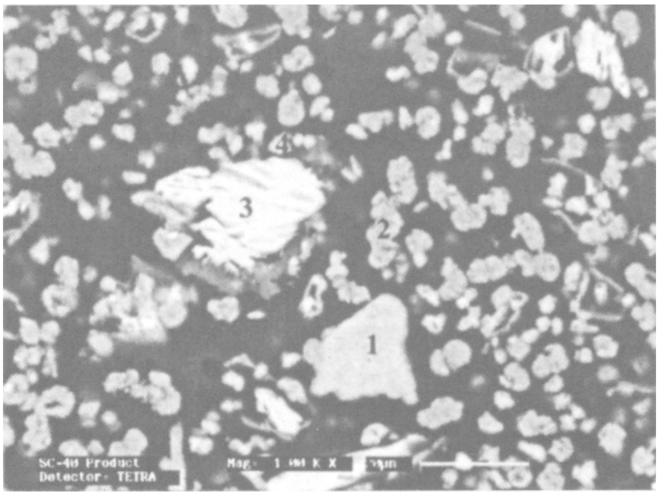

Figure 6 — BSE image of the SC-40 product.

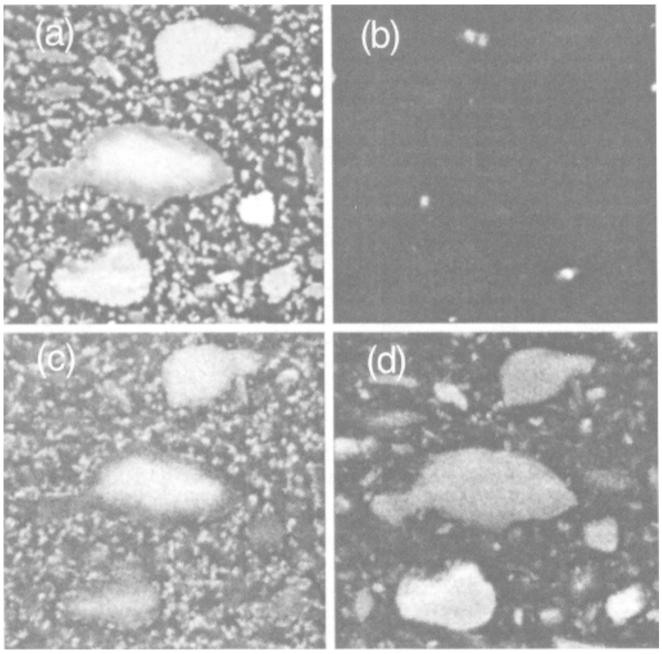

Figure 5 — (a) BSE image of SC-39 product (1,000 x) and (b), (c) and (d) X-ray maps for Fe, Mg and Si on SC-39 product, respectively.

was apparently sufficient for the magnesite crystals to grow into their characteristic rhombohedral structure, typical of the carbonate minerals (Fig. 4). This rhombohedral structure was not found in the reaction products for shorter duration tests. XRD analyses conducted on size fractions of the SC-11 product (Table 3) identified magnesite as a primary phase only in the -10-μm fraction. This size limitation appears to be universal. Recent studies indicate that carbonate precipitation occurs contemporaneously with silicate dissolution.

SC-39 serpentine reaction products. The character of the magnesite product does not appear to change with increasing extent of reaction. However, alteration of the original silicate mineral is much more pronounced. The reaction products from test SC-39, which achieved 83% stoichiometric conversion of heat pretreated serpentine to carbonate, are depicted in Fig. 5.

The large grain in the center of Fig. 5(a) shows a definite alteration rim. The X-ray maps suggest that this alteration rim is depleted in Mg (Fig. 5(c)), compared to the core of the grain. The Si concentration appears to be uniform throughout the grain (Fig 5(d)), suggesting that, as the Mg^{+2} is removed, the silica is not mobilized, producing a zone enriched in silica. The grain provides strong evidence for a shrinking core model for the reaction.

The large skeletal grain at lower left-center in Fig. 5(a) is composed primarily of silica. SEM-WDX microanalysis conducted on this grain reported a Mg/Si ratio of 3:4. This is half the theoretical Mg/Si ratio of 3:2 for serpentine, and this is lower than the theoretical ratios for either forsterite or enstatite. This grain could represent the primary fate of the silica, which may form masses of amorphous silica making up the matrix of the highly altered silicate grains. The Si X-ray map (Fig 5(d)) shows that fine particles (<10 μm) composed primarily of silica occur, but they are angular in shape compared to the more rounded magnesite particles. This may be due to attrition of the larger skeletal grains, rather than precipitation from solution. The latter would likely result in the formation of silica gel, which was a matter of concern early in the study. However, filtration rates of the product slurry have exceeded the rates that would be expected from silica gel-bearing slurry, providing further evidence that the silica is not dissolved.

The Fe X-ray map (Fig 5(b)) shows that the fine magnesite particles are virtually devoid of any Fe, which differs somewhat from the magnesite produced from the olivine feed. Most of the iron oxide contained in the serpentine feed is in the form of magnetite, which appears to remain relatively inert in the carbonation reaction.

SC-40 olivine reaction products. Test SC-40 achieved virtually the identical extent of reaction, i.e., 83% stoichiometric, as did test SC-39, although the latter utilized heat-treated serpentine as the feed rather than olivine. Test conditions were held constant between the two tests. Thus, it may be assumed that the heat-treatment step successfully produced an olivinelike feed material from the serpentine. This is supported by the XRD analyses (Table 3), which identified forsterite as the primary phase in the heat-treated serpentine product. This being said, the SC-40 reaction products should closely resemble those from SC-39.

Figure 6 is a BSE image of the SC-40 reaction product. The small (<10-μm) rounded particles dispersed throughout the view were identified as magnesite by SEM-WDX. The compositions of the larger grains in the view were of significant interest. A series of SEM-WDX point scans (Points 1 through 4 on Fig. 6) were collected to determine the C, Fe, Mg, O and Si concentration in the various particles. The results are shown in Table 5.

Table 5 — SEM-WDX microanalyses for SC-40 product. Point locations shown in Fig. 6.

	Atomic percent					
Point	**C**	**Fe**	**Mg**	**O**	**Si**	**Mg/Si**
1	3	0.3	20	63	13	1.5
2	26	ND	17	55	1	17
3	3	1.3	25	58	12	2.1
4	6	0.3	1	67	26	0.04

ND = Not detected

The analysis for Point 1 suggests that this is an altered olivine grain depleted in Mg, as indicated by the lower Mg/Si ratio, 3:2 compared to that for forsterite, 2:1. Point 2 provides a typical analysis for the magnesite particles. Silica content is very low, based on the Si analysis for Point 2, which supports the assertion made previously that silica does not report to the magnesite particles to any significant degree. The analysis for Point 3 indicates that the bright white grain is relatively unaltered olivine, at least at the core of the grain. A reaction rim extremely depleted in Mg is obvious at the lower portion of the grain. The grain represented by Point 4 is composed primarily of silica, indicative of the separate magnesite and silica particles that appear to make up the fine matrix of the sample. These small (5- to 10-µm) silica particles may result from attritioning of the coarser, skeletal grains of altered silicate described previously in the SC-39 reaction products.

Conclusions

An aqueous process for the direct carbonation of silicate minerals was developed as a method for CO_2 storage in solid form. Reaction rates were improved by the utilization of supercritical CO_2, with a P_{CO_2} of 115 to 185 atm, temperatures of 155° to 185°C and a solution chemistry including sodium bicarbonate and sodium chloride. Up to 78% stoichiometric conversion of the silicate mineral to the carbonate was achieved in 30 minutes under these conditions. The carbonation reaction product consists essentially of magnesite (~60% by weight), free silica (~25% by weight) and residual silicate (~15% by weight). Potential uses for the magnesite/silica product include soil amendments, replacing materials such as lime (CaO), limestone ($CaCO_3$) and/or dolomite [$(Ca,Mg)CO_3$]. The hydrophillic nature of the free silica may also improve soil water retention where necessary. The basic understanding of the mineral dissolution and carbonate precipitation reaction paths has been improved as a result of this characterization study.

Some important conclusions include the following:

- Conversion of the silicate to carbonate does not occur in the solid state, but appears to require mineral dissolution into the aqueous phase.
- Precipitation is the primary mechanism for carbonate formation and may occur contemporaneously with silicate dissolution.
- Alteration of the primary magnesium silicate minerals produces silica enriched, magnesium depleted intermediate products.
- While the mineral dissolution reaction is likely surface controlled, the formation of silica-enriched zones suggests the reaction may be diffusion limited.
- The formation of silica rims on the reaction surfaces may slow further dissolution. However, their formation appears to be limited in shorter-duration tests.
- Porous, skeletal grains with extremely high silica content were identified in the reaction products, suggesting that with continued removal of Mg^{+2} cations, the original silicate grains are converted to masses of amorphous silica.

Future studies are intended to investigate various mineral pretreatment options, alternative reactants, scale up to a continuous process and process economics.

References

Goff, F., Guthrie, G., Counce, D., Kluk, E., Bergfeld, D., and Snow, M., 1997, "Preliminary Investigations on the Carbon Dioxide Sequestering Potential of Ultramafic Rocks," Los Alamos, New Mexico, Los Alamos National Laboratory, LA-13328-MS.

Goff, F., Guthrie, G., Lipin, B., Fite, M., Chipera, S., Counce, D., Kluk, E., and Ziock, H., 2000, "Evaluation of Ultramafic Deposits in the Eastern United States and Puerto Rico as Sources of Magnesium for Carbon Dioxide Sequestration," Los Alamos, New Mexico, Los Alamos National Laboratory, LA-13694-MS, 36 pp.

Hunter, C.E., 1941, "Forsterite Olivine Deposits of North Carolina and Georgia," Raleigh, North Carolina, North Carolina Department of Conservation and Development, Bulletin 41.

IGCP (International Geological Program), 1977, "North American Ophiolites," R.G., Coleman and W.P. Irwin, eds., "Ophiolites of continents and comparable oceanic rocks," Portland, Oregon, State of Oregon, Dept. of Geology and Mineral Industries, Bulletin 95.

Lackner, K.S., Butt, D.P., Wendt, C.H., and Sharp, D.H., 1996, "Carbon dioxide disposal in solid form," *Proc. 21st International Conf. on Coal Utilization and Fuel Systems*, Coal Technology Association, Clearwater, Florida.

Lackner, K.S., Butt, D.P., and Wendt, C.H., 1997, "Magnesite Disposal of Carbon Dioxide," Los Alamos, New Mexico, Los Alamos National Laboratory, LA-UR-97-660.

O'Connor, W.K., Dahlin, D.C., Turner, P.C., and Walters, R.P., 1999, "Carbon dioxide sequestration by ex-situ mineral carbonation," *Technology*, Vol. 7S, pp. 115-123.

O'Connor, W.K., Dahlin, D.C., Nilsen, D.N., Rush, G.E., Walters, R.P., and Turner, P.C., 2000, "CO_2 storage in solid form: A study of direct mineral carbonation," *Proc. of the 5th International Conference on Greenhouse Gas Technologies*, Cairns, Australia, August 14-18, 7 pp.